

Vibration Suppression in a Two-Mass Drive System Using PI Speed Controller and Additional Feedbacks—Comparative Study

Krzysztof Szabat and Teresa Orłowska-Kowalska, *Senior Member, IEEE*

Abstract—In this paper, an analysis of control structures for the electrical drive system with elastic joint is carried out. The synthesis of the control structure with proportional–integral controller supported by different additional feedbacks is presented. The classical pole-placement method is applied. Analytical equations, which allow for calculating the control structure parameters, are given. The limitation of the design due to the number of degrees of freedom of the considered drive systems is shown. In order to damp the torsional vibration effectively, the application of the feedback from one selected state variable is necessary. In the literature, a large number of possible feedbacks have been reported. However, in this paper, it is shown that all systems with one additional feedback can be divided into three different groups, according to their dynamical characteristics. In addition, the system with two additional feedbacks is investigated. The comparison between considered structures is carried out. The simulation results are confirmed experimentally in the laboratory setup.

Index Terms—Elastic joint, electrical drive, pole-placement method, speed control, vibration suppression.

I. INTRODUCTION

A DRIVE SYSTEM is composed of a motor connected to a load machine through a shaft. In many cases, the joint is assumed to be stiff, yet in a number of applications, such as rolling-mill drives, robot arms, servo systems, textile drives, throttle systems, conveyor belts, and deep-space antenna drives, this assumption can lead to damaging oscillations [3], [9], [12]–[16], [22]. The speed oscillations decrease the system characteristics and product quality; the system can even lose stability.

The control problem is especially difficult when not all system state variables are measurable, which happens very often in industrial applications. The most popular classical cascade structure with the parameters of a proportional–integral (PI) speed controller adjusted according to the symmetrical criterion cannot damp the torsional vibrations effectively.

Manuscript received June 8, 2005; revised June 27, 2006. Abstract published on the Internet January 14, 2007. This work was supported by the National Scientific Research Committee (Poland) under Grant 3T10A 043 26 (2004–2006).

The authors are with the Institute of Electrical Machines, Drives and Measurements, Wrocław University of Technology, 50-372 Wrocław, Poland (e-mail: krzysztof.szabat@pwr.wroc.pl; teresa.orłowska-kowalska@pwr.wroc.pl).

Color versions of one or more of the figures in this paper are available online at <http://ieeexplore.ieee.org>.

Digital Object Identifier 10.1109/TIE.2007.892608

The simplest method to eliminate the oscillation problem, which occurs under the reference-speed changes, is a slow change of the reference velocity. Nevertheless, it causes the decrease of the drive system dynamics and does not protect against oscillations, which result while disturbance torque changes.

A method that can improve system performances exploits alternative tuning techniques for the classical cascade control structure (with a PI speed controller and the basic feedback from the motor speed), based on a suitable location of the closed-loop system poles. Three different pole locations with identical radius, damping coefficient, and real part were presented in [1]. In this paper the analytical guidelines were presented, that allow setting the controller parameters of every drive and examined the selected drive systems with respect to different mechanical parameters. A comparison of the system dynamics with different pole placements was made. The authors reported that the proposed locations are effective in the case of a large value of inertia ratio (defined as the ratio of the load to the motor moment of inertia). This method cannot damp the oscillations effectively when the inertia ratio has a comparatively small value (less than 1). Hence, the authors suggested the application of a proportional–integral–derivative controller. The derivative part D increased the inertia ratio of the system, virtually decreasing the moment of inertia of the motor. However, the authors claim that measurement noises can limit the value of part D in the real system; thus, the desired dynamical characteristics cannot be obtained.

In [2], Preitl and Precup analyzed another possible location of the closed-loop system poles. They proposed assigning the poles on the ellipse and reported that this location can provide more effective damping of the torsional vibrations than the location on the circle. However, this method is effective also only in the case when the inertia ratio has a relatively large value.

To improve the performances of the drive, the additional feedback loop from one selected state variable can be used. The additional feedback allows setting the desired value of the damping coefficient, yet the free value of resonant frequency cannot be achieved simultaneously. The additional feedbacks can be inserted to the electromagnetic-torque control loop or the speed control loop.

In [3], the additional feedback from the derivative of the shaft torque that was inserted into the electromagnetic-torque node was presented. The authors investigated the proposed

method and applied it to the two- and three-mass system. Nevertheless, the proposed estimator of the shaft torque is quite sensitive to measurement noises, so suppression of high-frequency vibrations is difficult; additionally, the dynamics of the system decreases. In [5], it was shown that in the case of the aforementioned structure, for the same value of the assumed damping coefficient, two different feedback gains can be designed, resulting in two different values of the resonant frequency of the system.

Another modification of the control structure results from inserting the additional feedback from the shaft torque. This type of feedback was utilized in [4]–[8]. The damping of the torsional vibration is reported to be successful. This structure is less sensitive to measurement noises than the former one since, in the analyzed system, the derivative of the shaft torque does not exist. In [6], the feedback from the difference between the motor and load speeds was utilized. Although the oscillations were successfully suppressed, the authors claim the loss of response dynamics and larger load impact effect. The additional feedback from the derivative of the load speed was proposed in [4], resulting in the same dynamical performance as for the previous control structure.

Another possible modification of the classical structure is based on the insertion of additional feedback to the speed control loop. In [5] and [7], the feedback from the load speed was applied. The authors argued that this feedback can ensure good dynamical characteristics and is able to damp vibrations effectively. The same results can be obtained by applying the feedback from the difference between the motor and load speeds.

The other torsional-vibration-suppression method relies on the additional feedback from the disturbance observer. This approach was proposed in [9]. In order to apply this method, the implementation of the fast disturbance torque observer is necessary. The time delay in the estimated state caused by the observer must be shorter than the vibration period. The compensation signal taken from the estimated disturbance torque is fed back to the electromagnetical torque node; the torsional vibrations are damped in this way. The authors reported good results. The more advanced approach was proposed in [10] and [11]. The control structure parameters were successfully designed to fulfill specifications such as load variations, backlash, and Coulomb friction in order to ensure very precise control.

The most advanced control structures, which ensure very good performance of the system, are based on the control structures with additional feedbacks from all state variables, i.e., shaft torque, load speed, and/or disturbance torque simultaneously. However, the direct feedbacks from these signals are very often impossible because additional measurements of these mechanical variables are difficult and costly, and reduce the system reliability. Therefore, the estimating problem of nonmeasurable variables attracted much attention [16]–[19]. In many papers, Luenberger observers were applied to the nonmeasurable state variable reconstruction. In the case of the linear system with nonchangeable parameters and a small value of measurement noises, this estimator can ensure good accuracy of the estimated states. However, in the presence of nonlinearity, parameter uncertainty, and high measurement noise level,

the performance of the Luenberger observer is nonsatisfactory [16], [17]. The dynamical characteristic improvement can be achieved by implementing the nonlinear Luenberger observer, as presented in [19]. However, this approach requires knowledge about the existing nonlinearity of the drive, which can be difficult in practice. For the system disturbed by measurement noises and with changeable parameters, the Kalman filter can ensure much better results of mechanical variable estimation than the Luenberger observer [16], [17]. It results from the fact that the Kalman filter algorithm relies directly on the parameter and measurement noises. In the presence of changeable parameters of the drive, the nonlinear Kalman filter can be used to estimate the correct value of these parameters [17], [18]. To ensure the proper work of the Kalman filter, there is a need to set the state and measurement covariance matrices correctly, which is a quite difficult task. Usually, the trial and error procedure is used. In [18], the genetic algorithms were applied to ensure the optimal setting of those matrices. The reconstruction of the full-state vector allowed implementing the state controller. This structure was presented in [16], [17], and [19]. Through the suitable selection of the closed-loop pole location, the dynamical characteristic of the system can be set freely. The torsional vibrations can be successfully damped.

In recent years, nonlinear and soft computing control methods have attracted much attention [20]–[25]. The application of the sliding [20] or the fuzzy control [21]–[24] increases the robustness of the drive system to parameter variations. The evolutionary algorithms can select the controller parameters to every desired control index [24]–[26]. The aforementioned techniques allowed obtaining better dynamical characteristics of the system, as compared to the classical ones, but they are not yet popular in industrial applications.

The control structures of electrical drives working in the industry are usually based on linear PI controllers. Despite a large number of publications, to our knowledge, there is a lack of papers that provide comprehensive and comparative results. Usually, one or two structures are examined and compared, and quite frequently analytical formulas allowing setting the controller parameters are missing. A survey of those control structures with analytical equations, which can provide adjustment of the control system parameter, is sought after.

Thus, the main goal of this paper is a systematic analysis and a presentation of the design guidelines for the speed control structures of the two-mass system with a PI speed controller that is supported by different additional feedbacks as well as a comparison of the dynamic properties of such structures. Aside from the structures mentioned in the introduction, in this paper, three additional structures were analyzed: two with feedback inserted to the torque loop and one with feedback inserted to the speed loop. Due to the limited length of this paper, the comparative studies were confined only to the control methods based on the additional feedbacks from the shaft and the load side. This paper does not include methods based on the feedback from the estimated load torque [9]–[11] or state controller [16], [17]. In addition, the description of the estimating methods of nonmeasurable variables [16]–[19] was not included in this paper. The theoretical investigation and the

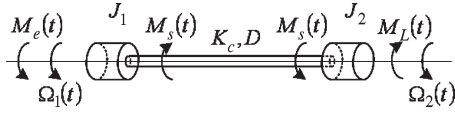


Fig. 1. Schematic diagram of the two-mass system.

simulation results presented in this paper were confirmed by experimental tests in a laboratory setup.

II. MATHEMATICAL MODEL OF THE SYSTEM

In technical papers, there exist many mathematical models that can be used for the analysis of the plant with elastic couplings. In many cases, the drive system can be modeled as a two-mass system, where the first mass represents the moment of inertia of the drive and the second mass refers to the moment of inertia of the load side. The mechanical coupling is treated as inertia free. The internal damping of the shaft is sometimes also taken into consideration. The schematic diagram of that model is presented in Fig. 1.

The system is described by the following state equation:

$$\frac{d}{dt} \begin{bmatrix} \Omega_1(t) \\ \Omega_2(t) \\ M_s(t) \end{bmatrix} = \begin{bmatrix} \frac{-D}{J_1} & \frac{D}{J_1} & \frac{-1}{J_1} \\ \frac{D}{J_2} & \frac{-D}{J_2} & \frac{1}{J_2} \\ K_c & -K_c & 0 \end{bmatrix} \begin{bmatrix} \Omega_1(t) \\ \Omega_2(t) \\ M_s(t) \end{bmatrix} + \begin{bmatrix} \frac{1}{J_1} \\ 0 \\ 0 \end{bmatrix} [M_e] + \begin{bmatrix} 0 \\ \frac{-1}{J_2} \\ 0 \end{bmatrix} [M_L] \quad (1)$$

where Ω_1 is the motor speed, Ω_2 is the load speed, M_e is the motor torque, M_s is the shaft (torsional) torque, M_L is the load torque, J_1 is the inertia of the motor, J_2 is the inertia of the load machine, K_c is the stiffness coefficient, and D is the internal damping of the shaft.

The aforementioned model is valid for the system where the moment of inertia of the shaft is much smaller than the moment of inertia of the motor and the load side. In other cases, the more extended model should be used, as the Rayleigh model of the elastic coupling or even a model with distributed parameters. The suitable choice of the mathematical model is a compromise between accuracy and calculation complexity. As can be concluded from the literature, nearly in all cases, the simplest inertia-shaft-free model has been used [1]–[12].

The resonant f_r and antiresonant f_{ar} frequencies of the two-mass system are defined as follows:

$$f_r = \frac{1}{2\pi} \sqrt{K_c \frac{J_1 + J_2}{J_1 J_2}} \quad f_{ar} = \frac{1}{2\pi} \sqrt{\frac{K_c}{J_2}}. \quad (2)$$

The value of the resonant frequency depends on the type of drive, can vary from a few hertz in a paper machine section [12] to dozens of hertz in a rolling-mill drive [15], and can exceed hundreds hertz in modern servo drives [14]. The value of the antiresonant frequency can be even ten times smaller than the resonant one in a dryer [12], but usually the difference is much smaller (smaller than two).

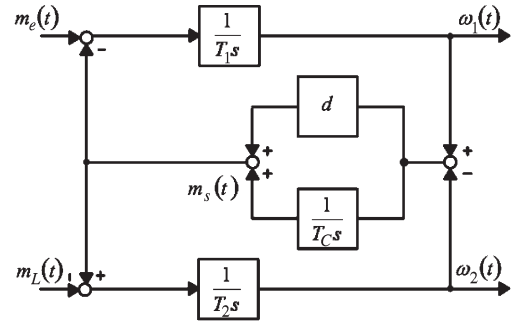


Fig. 2. Block diagram of the two-mass system.

To simplify the comparison of the dynamical performances of the drive systems of different powers, the mathematical model (1) was expressed in a per-unit system, using the following notation of new state variables:

$$\omega_1 = \frac{\Omega_1}{\Omega_N} \quad \omega_2 = \frac{\Omega_2}{\Omega_N} \\ m_e = \frac{M_e}{M_N} \quad m_s = \frac{M_s}{M_N} \quad m_L = \frac{M_L}{M_N} \quad (3)$$

where Ω_N is the nominal speed of the motor; M_N is the nominal torque of the motor; ω_1 and ω_2 are the motor and load speeds, respectively; m_e , m_s , and m_L are the electromagnetic, shaft, and load torques in the per-unit system, respectively.

The mechanical time constant of the motor T_1 and the load machine T_2 are, thus, given as

$$T_1 = \frac{\Omega_N J_1}{M_N} \quad T_2 = \frac{\Omega_N J_2}{M_N}. \quad (4)$$

The stiffness time constant T_c and internal damping of the shaft d can be calculated as follows:

$$T_c = \frac{M_N}{K_c \Omega_N} \quad d = \frac{\Omega_N D}{M_N}. \quad (5)$$

The block diagram of the two-mass system in the per-unit system is presented in Fig. 2 (where s is the Laplace operator).

III. CONTROL STRUCTURE ANALYSIS

A. General Remarks

A typical electrical drive system is composed of a power-converter-fed motor coupled to a mechanical system; microprocessor-based speed and torque controllers; and current, speed, and/or position sensors used for feedback signals. Usually, a cascade control structure containing two major control loops is used. The diagram of such system is presented in Fig. 3.

The inner control loop performs motor torque regulation and consists of a power converter, the electromagnetic part of the motor, and current sensor and respective current or torque controller. Therefore, this control loop is designed to provide

The closed-loop transfer functions from the reference speed to the motor and load speeds, respectively, for the control structure demonstrated in Fig. 4, are given by (6) and (7), shown at the bottom of the page (with the assumption that the optimized transfer function of the electromagnetic-torque control loop is equal to 1), where

$$G_r(s) = K_P + K_I \frac{1}{s} \quad (8)$$

is the transfer function of the PI controller.

B. Cascade Control Structure Without Additional Feedbacks

First, the control structure without additional feedback was considered. The characteristic equation of the analyzed system is given by

$$s^4 + s^3 \left(\frac{K_P}{T_1} \right) + s^2 \left(\frac{K_I}{T_1} + \frac{1}{T_1 T_c} + \frac{1}{T_2 T_c} \right) + s \left(\frac{K_P}{T_1 T_2 T_c} \right) + \frac{K_I}{T_1 T_2 T_c} = 0. \quad (9)$$

The desired polynomial of the system has the following form:

$$(s^2 + 2\xi\omega_0 s + \omega_0^2) (s^2 + 2\xi\omega_0 s + \omega_0^2) = 0 \quad (10)$$

where ξ is the damping coefficient and ω_0 is the resonant frequency of the closed-loop system.

Equation (10) can be rewritten as follows:

$$s^4 + s^3(4\xi\omega_0) + s^2(2\omega_0^2 + 4\xi^2\omega_0^2) + s(4\xi\omega_0^3) + \omega_0^4 = 0. \quad (11)$$

Through the comparison of relationships (9) and (11), the set of four equations is created, i.e.,

$$4\xi\omega_0 = \frac{K_P}{T_1} \quad (12a)$$

$$2\omega_0^2 + 4\xi^2\omega_0^2 = \frac{K_I}{T_1} + \frac{1}{T_1 T_c} + \frac{1}{T_2 T_c} \quad (12b)$$

$$4\xi\omega_0^3 = \frac{K_P}{T_1 T_2 T_c} \quad (12c)$$

$$\omega_0^4 = \frac{K_I}{T_1 T_2 T_c}. \quad (12d)$$

Solving the equation set (12), the parameters of the system, i.e., damping coefficient ξ and resonant frequency ω_0 , as well as the controller parameters, i.e., K_P and K_I , are obtained as

$$\xi = \frac{1}{2} \sqrt{\frac{T_2}{T_1}} \quad \omega_0 = \sqrt{\frac{1}{T_2 T_c}} \quad (13)$$

$$K_P = 2 \sqrt{\frac{T_1}{T_c}} \quad K_I = \frac{T_1}{T_2 T_c}. \quad (14)$$

The damping coefficient of the system depends on the inertia ratio defined as $R = T_2/T_1$. The decrease of the R value causes the larger and slowly damped oscillations in the system step response. In Fig. 5, the transients of the investigated control structure for system parameters $T_1 = 0.203$ s, $T_c = 0.0026$ s, $T_2 = 0.203$ s, and ($R = 1$) are presented.

The closed-loop system with the PI controller is of the fourth order. Because there are only two parameters of the PI controller, it is not possible to locate all the poles of the control structure without additional feedbacks independently. In order to improve the dynamical characteristics of the system, the application of additional feedbacks from selected state variables is necessary. As it was said before, the modified structures can be divided into three groups with respect to their dynamical characteristics. The parameters of all the systems presented here were calculated similarly with those of the system without additional feedbacks—using the pole-placement method.

C. Control Structures With Additional Feedbacks—Group A

This group includes the modified control structures with additional feedbacks from the shaft torque k_1 , from the derivative of the difference between the motor and load speeds k_2 , or from the derivative of the load speed k_3 .

First, the control structure with additional feedback from shaft torque k_1 was investigated. The damping coefficient and resonant frequency of this structure with the PI speed controller are the following:

$$\xi^{k_1} = \frac{1}{2} \sqrt{\frac{T_2(1+k_1)}{T_1}} \quad \omega_0^{k_1} = \sqrt{\frac{1}{T_2 T_c}}. \quad (15)$$

$$G_{\omega_1}(s) = \frac{\omega_1(s)}{\omega_r(s)}$$

$$= \frac{G_r(s)(s^2 T_2 T_c + 1)}{s^3 T_2 T_c (T_1 + k_2) + s^2 T_2 (G_r(s) T_c + G_r(s) k_7 + G_r(s) T_c k_8) + s (T_1 + T_2 (1 + k_1 + s T_c k_5) + k_3) + G_r(s) (1 + k_9) + k_6} \quad (6)$$

$$G_{\omega_2}(s) = \frac{\omega_2(s)}{\omega_r(s)}$$

$$= \frac{G_r(s)}{s^3 T_2 T_c (T_1 + k_2) + s^2 T_2 (G_r(s) T_c + G_r(s) k_7 + G_r(s) T_c k_8) + s (T_1 + T_2 (1 + k_1 + s T_c k_5) + k_3) + G_r(s) (1 + k_9) + k_6} \quad (7)$$

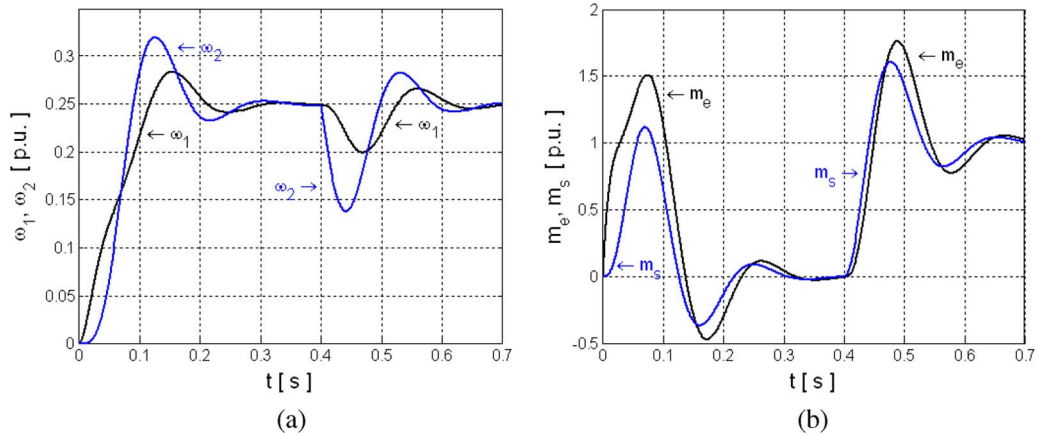


Fig. 5. Transients of the two-mass system without additional feedback: (a) motor and load speeds, and (b) electromagnetic and torsional torques.

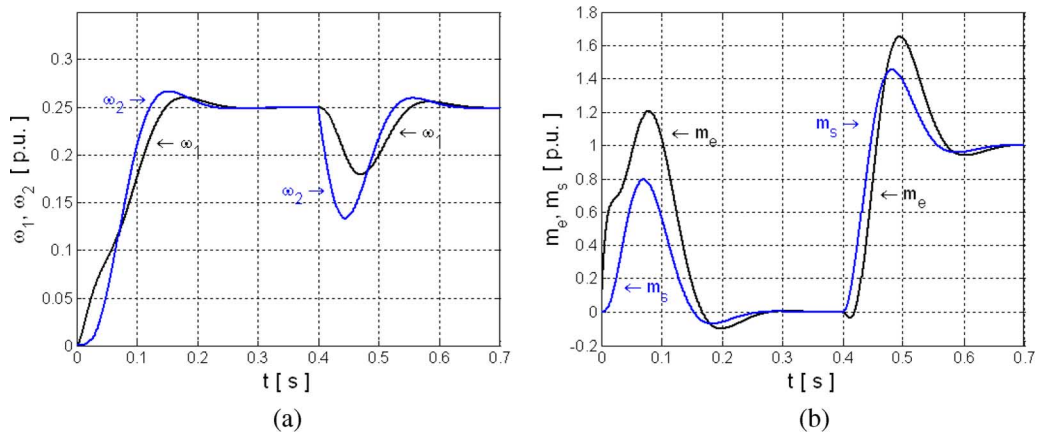


Fig. 6. Transients of the two-mass system for the control structures of group A with k_1 , k_2 , or k_3 feedbacks for $\xi_r = 0.7$: (a) motor and load speeds, and (b) electromagnetic and torsional torques.

The following equations allow setting the parameters of the feedback loop and the speed controller:

$$k_1 = \frac{4 \xi_r^2 T_1}{T_2} - 1 \quad K_P^{k_1} = 2 \sqrt{\frac{T_1(1+k_1)}{T_c}} \quad K_I^{k_1} = \frac{T_1}{T_2 T_c} \quad (16)$$

where ξ_r is the required damping coefficient of the system.

The damping coefficient and resonant frequency of the second system belonging to group A, with additional feedback from the derivative of the difference between two speeds k_2 , are

$$\xi^{k_2} = \frac{1}{2} \sqrt{\frac{T_2 - k_2}{T_1 + k_2}} \quad \omega_0^{k_2} = \sqrt{\frac{1}{T_2 T_c}} \quad (17)$$

The control structure parameters are given by

$$k_2 = \frac{T_2 - 4 \xi_r^2 T_1}{4 \xi_r^2 + 1}$$

$$K_P^{k_2} = 2 \sqrt{\frac{(T_1 + k_2)(T_2 - k_2)}{T_2 T_c}}$$

$$K_I^{k_2} = \frac{T_1 + k_2}{T_2 T_c} \quad (18)$$

For the next control structure with additional feedback from the derivative of the load speed k_3 , the damping coefficient and resonant frequency are

$$\xi^{k_3} = \frac{1}{2} \sqrt{\frac{T_2 + k_3}{T_1}} \quad \omega_0^{k_3} = \sqrt{\frac{1}{T_2 T_c}} \quad (19)$$

respectively.

The control structure parameters are determined in the following way:

$$k_3 = 4 \xi_r^2 T_1 - T_2 \quad K_P^{k_3} = 2 \sqrt{\frac{T_1(T_2 - k_3)}{T_2 T_c}} \quad K_I^{k_3} = \frac{T_1}{T_2 T_c} \quad (20)$$

In the three mentioned structures, the application of additional feedback (k_1 , k_2 , or k_3) increases the damping coefficient of the drive system, yet the resonant frequency remains unchanged [see, e.g., (15), (17), and (19)]. The systems have the same dynamical characteristics because, for every selected value of the damping coefficient, the characteristic equations of all three systems have identical forms. In Fig. 6, the transients of the considered control structures, for the assumed damping coefficient $\xi_r = 0.7$ and the same parameters of the drive, are presented.

D. Control Structures With Additional Feedbacks—Group B

Next, the structures of group B with additional feedbacks from the derivative of torsional torque k_4 , the difference between motor and load speeds k_5 , or the load speed k_6 , inserted to the torque node, were tested.

The damping coefficient and the resonant frequency of the system with additional feedback from the derivative of the shaft torque k_4 are

$$\xi^{k_4} = \sqrt{\frac{T_c + x}{4T_1T_c}(T_1 + T_2) + \frac{T_c}{4(T_c + x)} - \frac{1}{2}}$$

$$\omega_0^{k_4} = \sqrt{\frac{1}{T_2(T_c + x)}} \quad (21)$$

respectively, where x is the solution of the second-order equation defined by

$$x_{1,2} = \frac{-b \pm \sqrt{b^2 - 4ac}}{2a} \quad (22)$$

where

$$a = T_2^2(T_1 + T_2) \quad (23)$$

$$b = 2T_2^3T_c - 4\xi_r^2T_1T_2^2T_c \quad (24)$$

$$c = T_2^3T_c^2 - 4\xi_r^2T_1T_2^2T_c^2. \quad (25)$$

Depending on the parameters of the drive system, (22) can produce two, one, or no real solutions. It means that, for one assumed value of the damping coefficient ξ_r , the system can have a maximum two sets of parameters (B_1 and B_2) with different values of resonant frequency. The parameters of the considered control structure can be calculated using the following equations:

$$k_4 = xK_p^{k_4} \quad K_P^{k_4} = \frac{4\xi_r\omega_0^{k_4}T_1T_c}{T_c + x} \quad K_I^{k_4} = (\omega_0^{k_4})^4 T_1T_2T_c. \quad (26)$$

Then, the control structure with additional feedback from the difference between the motor and load speeds k_5 was investigated. The damping coefficient and the resonant frequency of the analyzed system are

$$\xi^{k_5} = \sqrt{\frac{(T_1 + T_2)(1 + x)}{4T_1} + \frac{1}{4(1 + x)^2} - \frac{1}{2}}$$

$$\omega_0^{k_5} = \sqrt{\frac{1}{T_2T_c(1 + x)}} \quad (27)$$

respectively.

Parameter x is obtained using (22) with the following coefficients:

$$a = T_1 + T_2 \quad (28)$$

$$b = -2T_1 - 4T_1\xi_r^2 \quad (29)$$

$$c = T_1. \quad (30)$$

The control structure parameters are, in this case,

$$k_5 = xK_p^{k_5} \quad K_P^{k_5} = \frac{4\xi_r\omega_0^{k_5}T_1}{(1 + x)} \quad K_I^{k_5} = (\omega_0^{k_5})^4 T_1T_2T_c. \quad (31)$$

Next, the control structure with additional feedback from the motor speed k_6 was investigated. The damping coefficient and resonant frequency of this structure with PI speed controller are the following:

$$\xi^{k_6} = \sqrt{\frac{(1 + x)^2T_1 + T_1 + T_2}{4T_1(1 + x)} - \frac{1}{2}} \quad \omega_0^{k_6} = \sqrt{\frac{(1 + x)}{T_2T_c}}. \quad (32)$$

In this case, parameter x is calculated using (22) with the following coefficients:

$$a = T_1 \quad (33)$$

$$b = -4T_1\xi_r^2 \quad (34)$$

$$c = T_2 - 4T_1\xi_r^2. \quad (35)$$

The following equations allow setting the parameters of the control structure:

$$k_6 = xK_p^{k_6} \quad K_P^{k_6} = 4\xi_r\omega_0^{k_6}T_1 \quad K_I^{k_6} = (\omega_0^{k_6})^4 T_1T_2T_c. \quad (36)$$

The considered systems have two sets of parameters B_1 and B_2 , which allow setting the desired value of the damping coefficient. In Fig. 7, the transients of the control structures of group B, for the assumed value of the damping coefficient $\xi_r = 0.7$, are demonstrated.

E. Control Structures With Additional Feedbacks—Group C

Group C consists of three structures with additional feedbacks from the derivative of shaft torque k_7 , the difference between the load and motor speeds k_8 , or the load speed k_9 . Unlike the previous two groups, the additional feedback is inserted to the speed node.

First, the control structure with additional feedback from the derivative of the torsional torque k_7 was examined. The system damping coefficient and resonant frequency are

$$\xi^{k_7} = \frac{1}{2} \sqrt{\frac{(T_1 + T_2)(T_c + k_7)}{T_1T_c} - 1} \quad \omega_0^{k_7} = \sqrt{\frac{1}{T_2(T_c + k_7)}}. \quad (37)$$

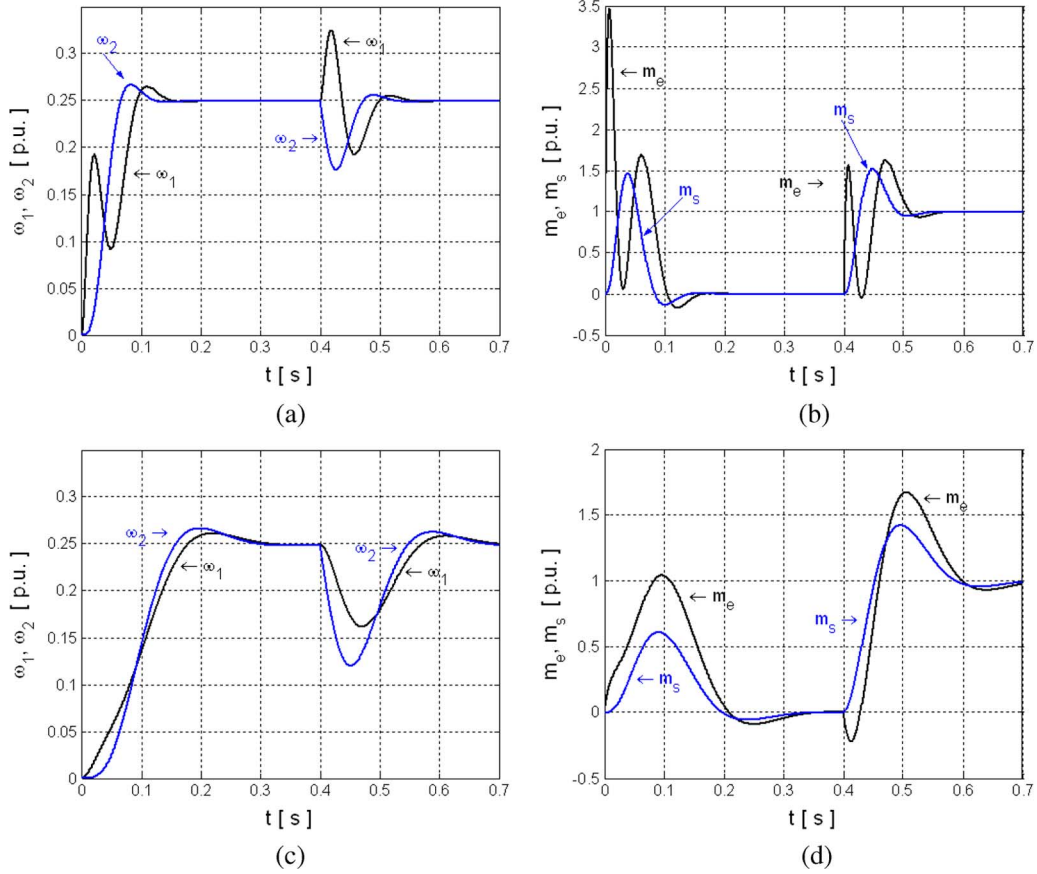


Fig. 7. Transients of the two-mass system for the control structures of group B with k_4 , k_5 , or k_6 feedbacks for the (a) and (b) larger and (c) and (d) smaller values of system resonant frequency for $\xi_r = 0.7$: (a) and (c) motor and load speeds, and (b) and (d) electromagnetic and torsional torques.

The control structure parameters are determined in the following way:

$$\begin{aligned} k_7 &= \frac{(4\xi_r^2 + 1)T_1T_c}{T_1 + T_2} - T_c \\ K_P^{k_7} &= 4\xi_r(\omega_0^{k_7})^3 T_1T_2T_c \\ K_I^{k_7} &= (\omega_0^{k_7})^4 T_1T_2T_c. \end{aligned} \quad (38)$$

Next, the control structure with additional feedback from the difference between motor and load speed k_8 was tested. The damping coefficient and resonant frequency are

$$\xi^{k_8} = \frac{1}{2} \sqrt{\frac{T_1k_8 + T_2(1+k_8)}{T_1}} \quad \omega_0^{k_8} = \sqrt{\frac{1}{(1+k_8)T_2T_c}} \quad (39)$$

respectively.

The control structure parameters are given by

$$\begin{aligned} k_8 &= \frac{\xi_r^2 4T_1 - T_2}{T_1 + T_2} \\ K_P^{k_8} &= \frac{4\xi_r\omega_0^{k_8}T_1}{1+k_8} \\ K_I^{k_8} &= \frac{T_1}{(1+k_8)^2 T_2T_c}. \end{aligned} \quad (40)$$

In the end, the system with additional feedback from the load speed k_9 was considered. The damping coefficient and resonant frequency of this system are defined as

$$\xi^{k_9} = \frac{1}{2} \sqrt{\frac{T_1 + T_2}{T_1(1+k_9)}} - 1 \quad \omega_0^{k_9} = \sqrt{\frac{1+k_9}{T_2T_c}}. \quad (41)$$

The parameters of the control structure can be calculated based on the following equations:

$$\begin{aligned} k_9 &= \frac{T_1 + T_2}{T_1(4\xi_r^2 + 1)} - 1 \\ K_P^{k_9} &= 4\xi_r\omega_0^{k_9}T_1 \\ K_I^{k_9} &= \frac{T_1(1+k_9)}{T_2T_c}. \end{aligned} \quad (42)$$

The reference value of the last system should be set according to the following formula: $\omega_r^* = \omega_r(1+k_9)$. All three systems have the same dynamical characteristics. The transients of the drive system for the assumed damping coefficient $\xi_r = 0.7$ are shown in Fig. 8.

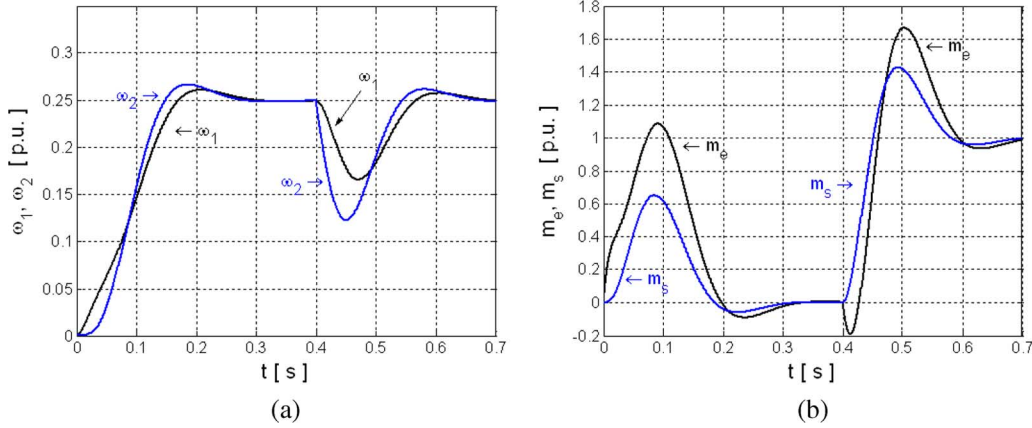


Fig. 8. Transients of the two-mass system for the control structures of group C with k_7 , k_8 , or k_9 feedbacks for $\xi_r = 0.7$: (a) motor and load speeds, and (b) electromagnetic and torsional torques.

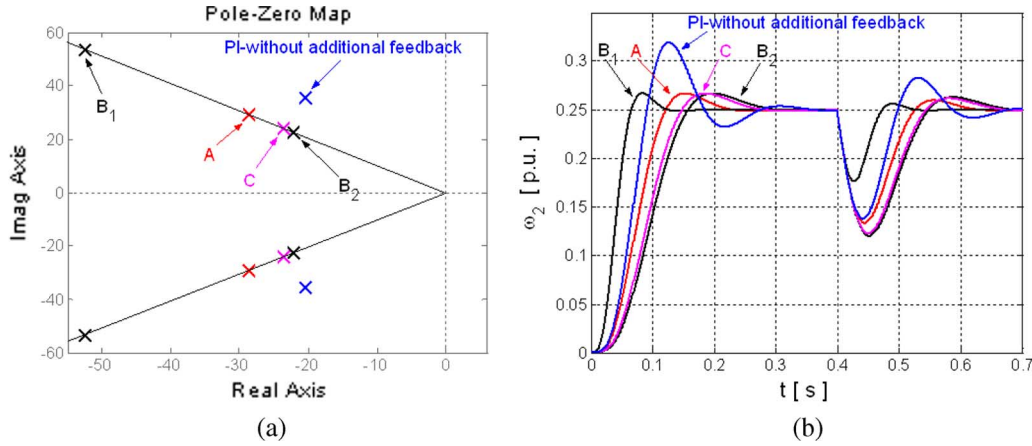


Fig. 9. (a) Closed-loop pole location and (b) load-speed transient of all considered systems.

F. Comparison of Dynamical Performance of Control Structures

In Fig. 9(a), the closed-loop pole loci of all considered control systems are presented. These systems are of the fourth order, and the presented poles are double. The closed-loop pole location of the system without additional feedback depends only on the mechanical parameters of the drive [according to (5)]. The system poles are situated relatively close to the imaginary axis. The response of the drive system has quite a large overshoot and settling time.

The closed-loop pole location of the system with one additional feedback depends on the assumed damping coefficient, which, in each case, was set to $\xi_r = 0.7$.

The closed-loop poles of the system from group B (in this case, B_1) have the highest value of the resonant frequency, when the additional feedback coefficient (k_4 , k_5 , or k_6) has a negative value. The rising time of the speed response of the mentioned drive is approximately twice as short as that of the remaining systems. The next faster system is the control structure belonging to group A. The dynamical characteristics of the remaining structures (group C and group B_2) are quite similar. In Fig. 9(b), the load-speed transients of all considered systems are presented. The shape of the curves confirms the closed-loop pole location analysis.

G. Control Structure With Two Feedbacks

To obtain a free design of the control structure parameters, i.e., the resonant frequency and damping coefficient, the application of two feedbacks from different groups is necessary. The type of selected feedback from a particular group is not significant because, as was shown before, feedbacks belonging to the prescribed group give, in fact, the same results. Because a large number of possibilities for the choice of two different feedbacks exist, only one case was considered here.

The system with additional feedbacks from the derivative of the difference between speeds (in group A, k_2) and from the difference between the motor and load speeds (in group C, k_8) was investigated. The system resonant frequency and damping coefficient are determined as follows:

$$\zeta^{k_2+k_8} = \frac{1}{2} \sqrt{\frac{(T_1 + T_2)(1 + k_8)}{4(T_1 + k_2)} - \frac{1}{4}}$$

$$\omega_0^{k_2+k_8} = \sqrt{\frac{1}{(1 + k_8)T_2T_c}} \quad (43)$$

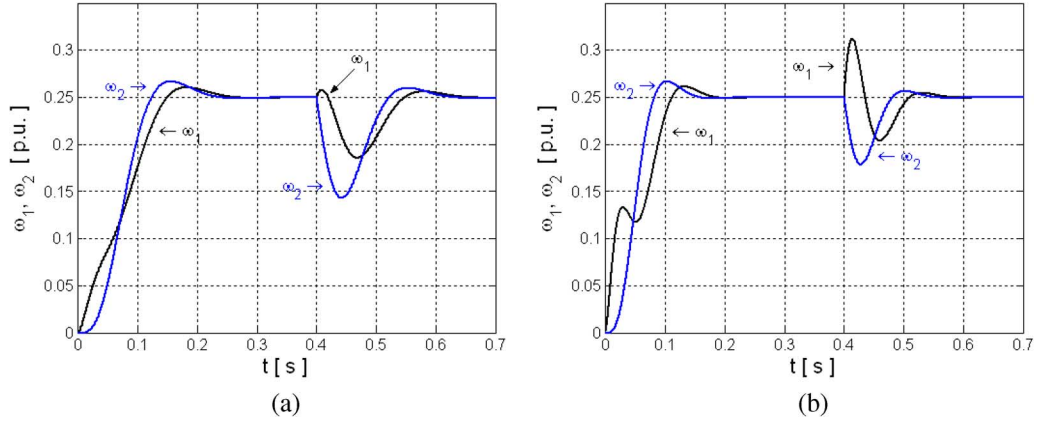


Fig. 10. Speed transients of the two-mass system with two additional feedbacks k_2 and k_8 for $\xi_r = 0.7$ and two different values of the resonant frequency (a) $\omega_r = 40 \text{ s}^{-1}$ and (b) $\omega_r = 60 \text{ s}^{-1}$.

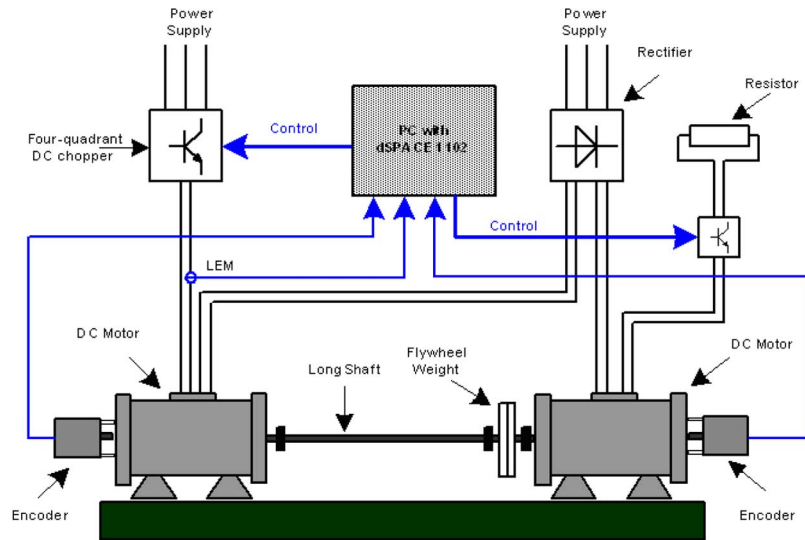


Fig. 11. Schematic diagram of experimental setup.

The additional feedback coefficients should be calculated in the following way:

$$k_8 = \frac{1}{(\omega_r^{k_2+k_8})^2 T_2 T_c} - 1 \quad k_2 = \frac{(T_1 + T_2)(1 + k_7)}{(4 \xi_r)^2 + 1} - T_1 \quad (44)$$

where ω_r is the required resonant frequency of the system.

Thus, the parameters of the PI controller are calculated using the following expressions:

$$K_P^{k_2+k_8} = \frac{4 \xi_r \omega_r^{k_2+k_8} (T_1 + k_2)}{1 + k_8}$$

$$K_I^{k_2+k_8} = T_2 T_c (T_1 + k_2) (\omega_r^{k_2+k_8})^4. \quad (45)$$

In Fig. 10, the system speed transients for two required values of the resonant frequency and the damping coefficient $\xi_r = 0.7$ are presented. It is seen that the system dynamics can be programmed freely.

IV. RESULTS OF EXPERIMENTAL TESTS

All theoretical considerations were confirmed experimentally. The laboratory setup, which is presented in Fig. 11, was composed of a dc motor driven by a four-quadrant chopper. The motor was coupled to a load machine by an elastic shaft (a steel shaft with a diameter of 5 mm and a length of 600 mm). The load machine was also a dc motor. The motors had a nominal power of 500 W each. The speed and position of both motors were measured by incremental encoders (5000 pulse/rotation). The mechanical system had a natural frequency of approximately 9.5 Hz. The control and estimation algorithms were implemented by a digital signal processor using the dSPACE software. To avoid the limitation of the electromagnetic torque, the reference value was set to 25% of the nominal speed.

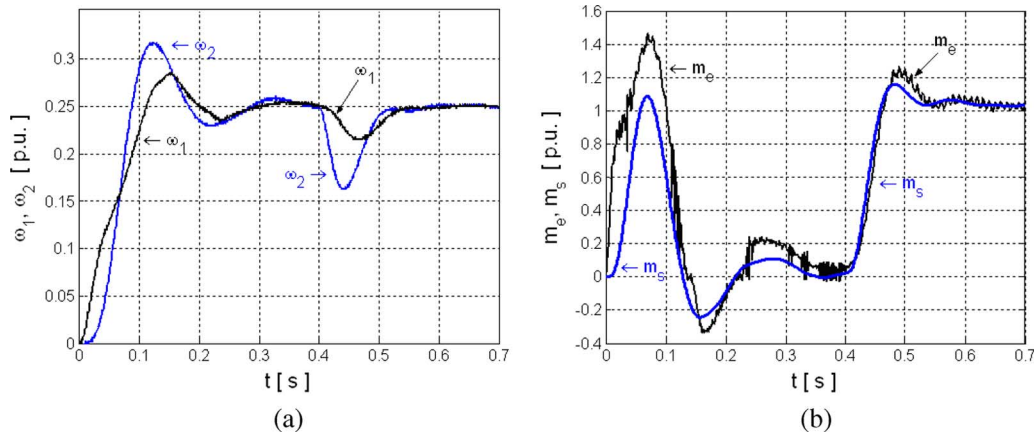


Fig. 12. Experimental transients of the system without additional feedback: (a) motor and load speeds, and (b) electromagnetic and torsional torques.

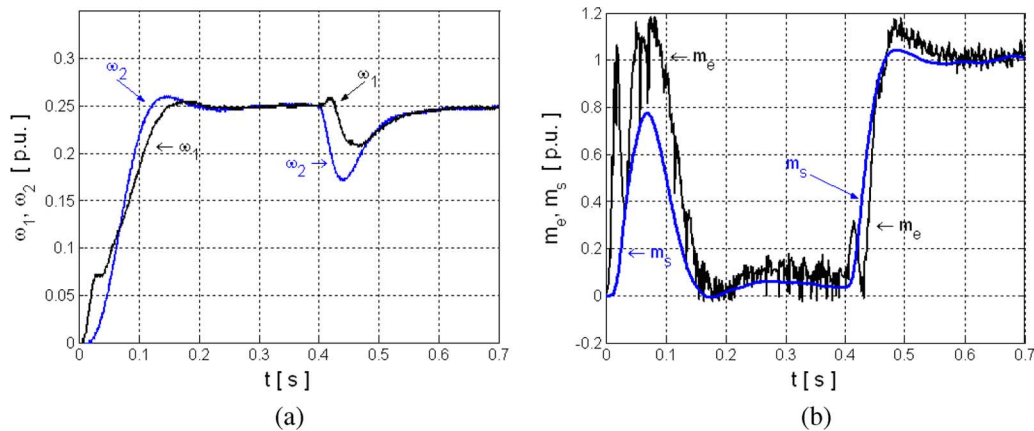


Fig. 13. Experimental transients of the system with additional feedback from the derivative of the difference between speeds k_2 (group A) for $\xi_r = 0.7$: (a) motor and load speeds, and (b) electromagnetic and torsional torques.

The first considered control structure was the system with a PI controller without additional feedback, which was designed according to (13) and (14). As shown in Fig. 12(a), the load speed of the system has a large overshoot and a quite long settling time. The maximum value of electromagnetic torque is about 1.4 the value of the nominal torque [Fig. 12(b)].

Next, the system with additional feedback from the derivative of the difference between motor and load speeds k_2 was investigated (the group A). The damping coefficient of the control structure was set, similarly as in simulation tests, to $\xi_r = 0.7$. The transients of the system fulfill the assumed dynamical characteristics; the overshoot is small, and the torsional vibrations are damped successfully (Fig. 13).

Then, the control structure with additional feedback from the difference between speeds k_5 was examined (group B). This system has two sets of parameters, which allow setting the desired value of the damping coefficient. First, the drive system with a larger value of resonant frequency was investigated. In Fig. 14(a) and (b), the system transients are presented. The responses to the speed reference change as well as the load torque change are very fast, which is clearly seen in the motor-speed transient. However, the maximum value of electromagnetic torque during startup was four times larger than the nominal one.

Then, the drive system with a smaller value of resonant frequency was tested. The system transients are shown in Fig. 14(c) and (d). The load speed has a small (assumed) value of overshoot; in this case, the value of resonant frequency was much smaller, and the electromagnetic torque under transients does not reach values that are larger than the nominal one.

The next examined system was the structure with additional feedback from the difference between the motor and load speeds inserted in the speed node (k_8 for group C). In Fig. 15, the transients of the analyzed system are presented. The load-speed overshoot has a small value, resulting from the assumed value of the system damping coefficient, similarly as in simulation tests.

Finally, the control structure with two additional feedbacks from the derivative of the difference between speeds k_2 and the difference between the motor and load speeds k_8 was tested. The system with two feedbacks ensures free design of mechanical characteristics, which is illustrated in Fig. 16.

The presented results confirmed the analytical investigations and simulation tests. The slight difference between the real and simulation transients comes from the fact that, in real-system nonlinearities such as friction, the nonlinear characteristic of the shaft, which has been neglected in the simulation, exists, and the perfect derivative part applied in some structures was

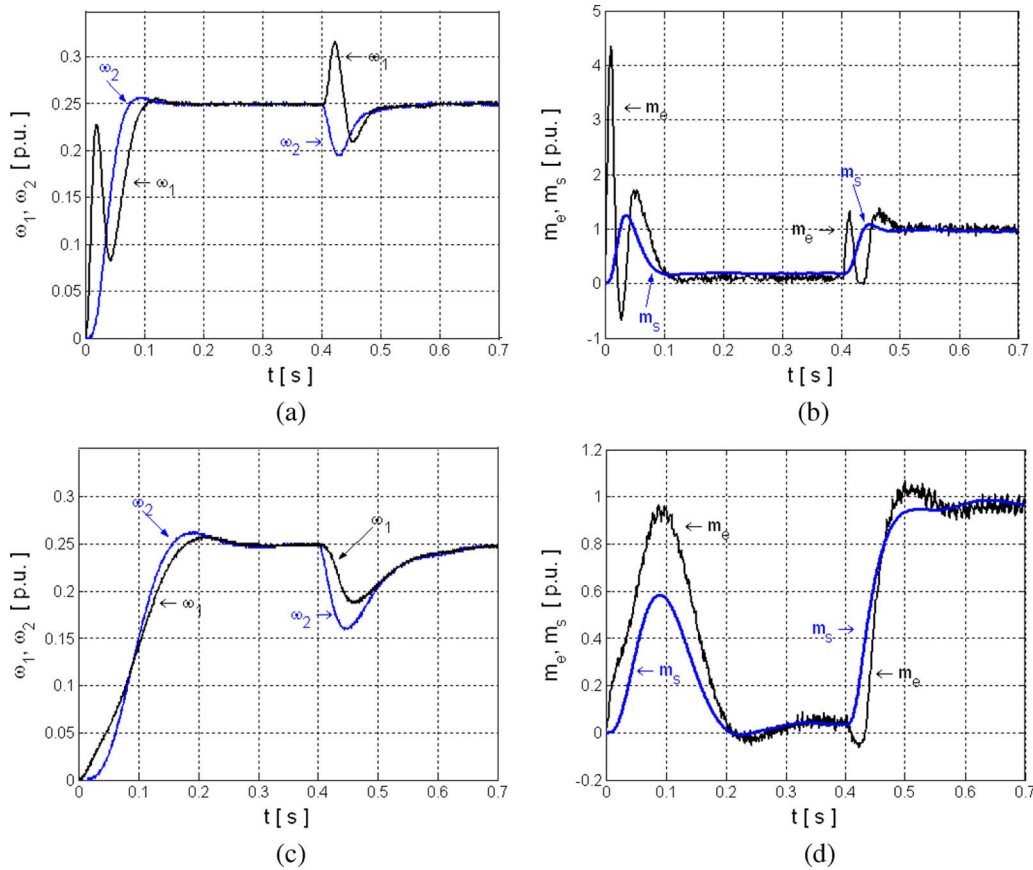


Fig. 14. Experimental transients of the system with additional feedback from the difference between speeds k_5 in (a) and (b) group B_1 and (c) and (d) group B_2 for $\xi_r = 0.7$: (a) and (c) motor and load speeds, and (b) and (d) electromagnetic and torsional torques.

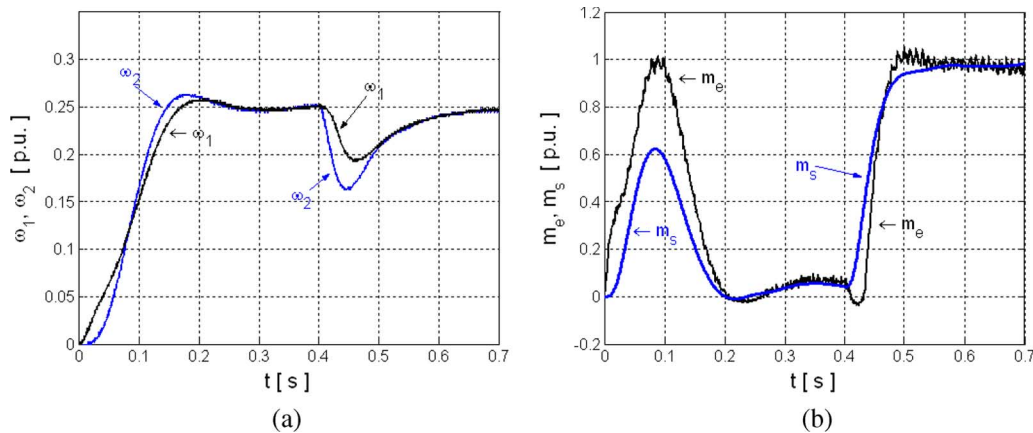


Fig. 15. Experimental transients of the system with additional feedback from the difference between speeds k_8 (group C) for $\xi_r = 0.7$: (a) motor and load speeds, and (b) electromagnetic and torsional torques.

replaced with a pseudoderivative term with small (3 ms) time constant.

V. CONCLUSION

In this paper, different cascade control structures with additional feedbacks for the electrical drive system with a flexible connection were investigated. To calculate the control system parameters, the classical pole-placement method was

implemented. The performances of the control structure without additional feedback depend on the mechanical parameters of the considered drive and are rather poor. This results from the fact that the system is of the fourth order and there are only two controller parameters (K_I , K_P), which cannot form the desired damping coefficient and resonant frequency simultaneously. In order to damp the torsional vibrations effectively, the application of one additional feedback is necessary. Resulting from the review of the literature, the application of different

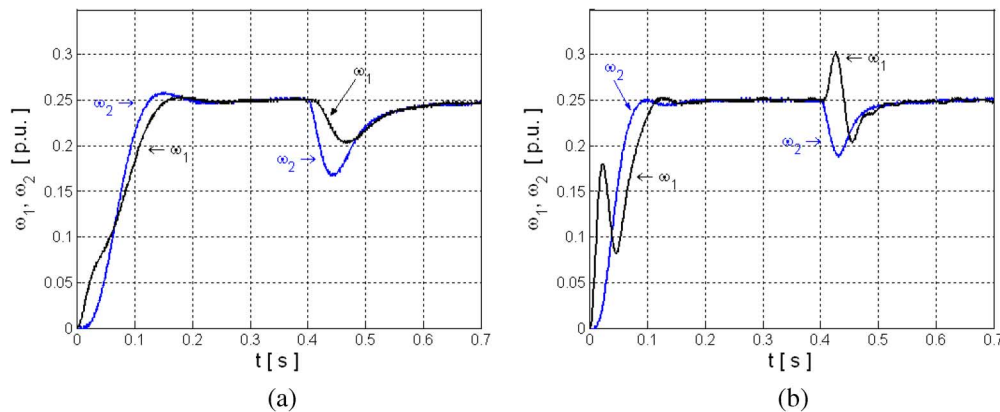


Fig. 16. Experimental speed transients of the system with additional feedbacks from group A (k_2) and group C (k_8) for $\xi_r = 0.7$ and two different values of the resonant frequency (a) $\omega_r = 40$ and (b) $\omega_r = 60$.

feedbacks is possible. Despite of the large number of existing structures, the systems with one additional feedback can be divided into three different groups, according to their dynamical characteristic. It was proved in this paper that all structures within a certain group have the same pole placement and, thus, the same transient responses.

The structures with one additional feedback ensure setting the desired value of the damping coefficient, yet the required value of the resonant frequency cannot be adjusted at the same time. The best dynamical characteristics are obtained in the control structure from group B_1 . The resonant frequency of that system is about twice higher than of those the remaining structures.

If the design specifications require the free setting of the damping coefficient and resonant frequency simultaneously, the application of two additional feedbacks is necessary. Because the control structure with the PI controller and two additional feedbacks has four parameters and the system is of the fourth order, the closed-loop poles can be placed in every desired position. The theoretical assumptions and analysis developed in this paper were confirmed by simulation and experimental tests.

REFERENCES

- [1] G. Zhang and J. Furusho, "Speed control of two-inertia system by PI/PID control," *IEEE Trans. Ind. Electron.*, vol. 47, no. 3, pp. 603–609, Jun. 2000.
- [2] S. Preitl and R. E. Precup, "An extension of tuning relations after symmetrical optimum method for PI and PID controllers," *Automatica*, vol. 35, no. 10, pp. 1731–1736, 1999.
- [3] K. Sugiura and Y. Hori, "Vibration suppression in 2- and 3-mass system based on the feedback of imperfect derivative of the estimated torsional torque," *IEEE Trans. Ind. Electron.*, vol. 43, no. 1, pp. 56–64, Feb. 1996.
- [4] G. Zhang, "Comparison of control schemes for two-inertia system," in *Proc. Int. Conf. PEDS*, Hong Kong, 1999, pp. 573–578.
- [5] K. Szabat and T. Orłowska-Kowalska, "Comparative analysis of different PI/PID control structures for two-mass system," in *Proc. 7th Int. Conf. Optim. Electr. and Electron. Equipment, OPTIM*, Brasov, Romania, 2004, pp. 97–102.
- [6] J. M. Pacas, J. Armin, and T. Eutebach, "Automatic identification and damping of torsional vibrations in high-dynamic-drives," in *Proc. ISIE*, Choluta-Puebla, Mexico, 2000, pp. 201–206.
- [7] K. Gierlotka, P. Zalesny, and M. Hyla, "Additional feedback loops in the drives with elastic joints," in *Proc. Int. Conf. EDPE*, Košice, Slovakia, 1996, vol. 2, pp. 558–563.
- [8] T. O'Sullivan, C. C. Bingham, and N. Schofield, "High-performance control of dual-inertia servo-drive systems using low-cost integrated SAW torque transducers," *IEEE Trans. Ind. Electron.*, vol. 53, no. 4, pp. 1226–1237, Jun. 2006.
- [9] T. Ohmahe, T. Matsuda, M. Kanno, K. Saito, and T. Sukegawa, "A microprocessor-based motor speed regulator using fast-response state observer for reduction of torsional vibration," *IEEE Trans. Ind. Appl.*, vol. IA-23, no. 5, pp. 863–871, Sep. 1987.
- [10] Y. Hori, H. Sawada, and Y. Chun, "Slow resonance ratio control for vibration suppression and disturbance rejection in torsional system," *IEEE Trans. Ind. Electron.*, vol. 46, no. 1, pp. 162–168, Feb. 1999.
- [11] S. Komada, H. Imama, K. Yubai, and T. Hori, "Suppression of limit cycle and improvement of robust performance in two-mass resonant systems with nonlinearity," in *Proc. 27th Annu. IEEE IECON*, 2001, pp. 1704–1709.
- [12] M. A. Valenzuela, J. M. Bentley, and R. D. Lorenz, "Evaluation of torsional oscillations in paper machine sections," *IEEE Trans. Ind. Appl.*, vol. 41, no. 2, pp. 493–501, Mar./Apr. 2005.
- [13] J. Arellano-Padilla, G. M. Asher, and M. Sumner, "Control of a dynamometer for dynamic emulation of mechanical loads with stiff and flexible shafts," *IEEE Trans. Ind. Electron.*, vol. 53, no. 4, pp. 1250–1260, Jun. 2006.
- [14] S. N. Vukosovic and M. R. Stojic, "Suppression of torsional oscillations in a high-performance speed servo drive," *IEEE Trans. Ind. Electron.*, vol. 45, no. 1, pp. 108–117, Feb. 1998.
- [15] R. Dhaoui, K. Kubo, and M. Tobise, "Two-degree-of-freedom robust speed controller for high-performance rolling mill drivers," *IEEE Trans. Ind. Appl.*, vol. 29, no. 5, pp. 919–926, Sep./Oct. 1993.
- [16] J. K. Ji and S. K. Sul, "Kalman filter and LQ based speed controller for torsional vibration suppression in a 2-mass motor drive system," *IEEE Trans. Ind. Electron.*, vol. 42, no. 6, pp. 564–571, Dec. 1995.
- [17] S. Beineke, F. Schütte, and H. Grotstollen, "Comparison of methods for state estimation and on-line identification in speed and position control loops," in *Proc. Int. Conf. EPE*, 1997, pp. 3.364–3.369.
- [18] K. Szabat, T. Orłowska-Kowalska, and K. Dyrzcz, "Extended Kalman filters in the control structure of two-mass drive system," *Bull. Pol. Acad. Sci. Tech. Sci.*, vol. 54, no. 3, pp. 315–325, 2006.
- [19] K. Peter, I. Schoeling, and B. Orlik, "Robust output-feedback H_∞ control with a nonlinear observer for a two-mass system," *IEEE Trans. Ind. Appl.*, vol. 39, no. 3, pp. 637–644, May/June 2003.
- [20] P. Korondi, H. Hashimoto, and V. Utkin, "Direct torsion control of flexible shaft in an observer-based discrete-time sliding mode," *IEEE Trans. Ind. Electron.*, vol. 45, no. 2, pp. 291–296, Apr. 1998.
- [21] Y. C. Hsu, G. Chen, and H. X. Li, "A fuzzy adaptive variable structure controller with applications to robot manipulators," *IEEE Trans. Syst., Man, Cybern. B, Cybern.*, vol. 31, no. 3, pp. 331–340, Jun. 2001.
- [22] K. Fischle and D. Schröder, "Stable model reference neurocontrol for electric drive systems," in *Proc. Int. Conf. EPE*, 1997, pp. 2.432–2.437.
- [23] T. Orłowska-Kowalska and K. Szabat, "Control of the drive system with stiff and elastic couplings using adaptive neuro-fuzzy approach," *IEEE Trans. Ind. Electron.*, vol. 54, no. 1, pp. 228–240, Jan./Feb. 2007.
- [24] F. Janabi-Sharifi and J. Liu, "Design of a self-adaptive fuzzy tension controller for tandem rolling," *IEEE Trans. Ind. Electron.*, vol. 52, no. 5, pp. 1428–1438, Oct. 2005.

- [25] K. Itoh, M. Iwasaki, and N. Matsui, "Optimal design of robust vibration suppression controller using genetic algorithms," *IEEE Trans. Ind. Electron.*, vol. 51, no. 5, pp. 947–953, Oct. 2004.
- [26] M. Iwasaki, M. Miwa, and N. Matsui, "GA-based evolutionary identification algorithm for unknown structured mechatronic systems," *IEEE Trans. Ind. Electron.*, vol. 52, no. 1, pp. 300–305, Feb. 2005.



Krzysztof Szabat received the M.Sc. and Ph.D. degrees from Wroclaw University of Technology, Wroclaw, Poland, in 1999 and 2003, respectively.

Since 1999, he has been a member of the Academic Staff of the Electrical Drives Control Chair, Institute of Electrical Machines, Drives, and Measurements, Wroclaw University of Technology. He is the author or coauthor of more than 50 journal and conference papers. His research interests include applications of control theory, artificial intelligence methods, and microprocessor techniques applied to electrical drives control.



Teresa Orłowska-Kowalska (M'93–SM'04) received the Ph.D. and D.Sc. degrees from Wroclaw University of Technology, Wroclaw, Poland, in 1976 and 1990, respectively.

Since 1993, she has been a Professor of electrical engineering and the Head of the Electrical Drives Control Chair at the Institute of Electrical Machines, Drives, and Measurements, Wroclaw University of Technology. She is the author or coauthor of more than 200 journal and conference papers, two textbooks, one book (*Sensorless Control of Induction Motor Drives*, Academic, 2003), and five chapters in monographs. Her research interests include mathematical modeling and microprocessor control of electrical drives and power electronic systems, application of modern control methods to electrical drives, and state estimation of induction motors using state observers, Kalman filters, and neural networks. In the last few years, her main research interests have included neural networks and fuzzy-logic techniques applied to electrical drives control.

Dr. Orłowska-Kowalska has been a member of the Electrical Engineering Committee of the Polish Academy of Science since 1996 and is a member of the European Power Electronics Association, CIGRE, and international steering committees of a few well-known European conferences.